JEASD

THE EFFECT OF MOISTURE CONTENT ON ELECTRICAL PROPERTIES OF SELECTED SOFTWOODS; CEDAR, JUNIPER, AND PINE

Sinan Saeed Jasim Alsaadi[1*], Atalay Kocakusak[2], and Selcuk Helhel[3]

[1,2] *Department of Electrical and Electronics Engineering, Engineering Faculty, Akdeniz University, 07058, Antalya, Turkey*
[3]*Industrial and Medical-Based Microwave Research Center EMUMAM, Akdeniz University, 07058, Antalya, Turkey*
[1]https://orcid.org/0009-0009-1985-3197
[2]https://orcid.org/0000-0002-2457-4426
[3]https://orcid.org/0000-0002-1401-3297

Abstract: Natural woods as a raw material have been taking a considerable interest topic by industries such as the forest industry, furniture manufacturing, and nowadays suitable electronics. One of the most essential steps of manufacturing for those industry purposes is RF heating/drying of raw wood material nowadays. However, knowing the electrical properties, such as the dielectric constant of wood-based material before processing is tremendously important. It is well-known that the moisture content and density levels of material directly affect the dielectric properties. Moisture and density conditions are different in each material because it's related directly to the absorption and affection of material towards moisture sources. Therefore, in this study of wood material under varying conditions, proper empiric models have been generated to express this relationship. This study is based on three different softwood specimens widely used in the forest industry. The dielectric properties were determined in the frequency range of 2.17 GHz-6.0 GHz as a function of moisture content and density for wood species. Each measurement contains 500 raw data points; a vector network analyzer collected 49,500 S-parameter data. Each wood specimen consists of six samples; the average of data obtained from these samples was considered as a dielectric measure for the examined wood specimen. The proposed empiric models have RMSE better than 0.05 for the relation between loss tangent and density, while the proposed empiric models for dielectric permittivity have better than 0.90 with density relation, which is considered an acceptable ratio for model generation.

Keywords: Empiric mathematical models; loss tangent; relative dielectric constant; wood physics

1. Introduction

In recent years, there has been an interest in using natural materials in industry and manufacturing by studying the physical properties of such raw materials through different conditions. Embedded into the analyses of the electromagnetic field and material interaction is required to change the physical properties of the material and to gain new features by making use of its chemical properties. However, these processes do not take into account the field of industry application in manufacturing, communication, and remote sensing. Therefore, the electrical properties of the material should be known clearly. However, such knowledge of the physical properties of wooden material will allow us to gain experience with the tree trunk chemical matter

*Corresponding Author:
20185191006@ogr.akdeniz.edu.tr

type and the amount of dissolved substance. In contrast, knowing the electrical properties of any wood structure is of great importance not only for applications that depend on heating/drying systems that are used in woodworking technologies but also for non-destructive sensor studies, including remote sensing [1]. The most fundamental quantities for the interaction of electromagnetic waves with materials are the quantities related to reflection "Γ", absorption "A", and transmission "τ" coefficients. These quantities are measured using vector network analyzers (VNA) by collecting scattering parameters (S_{11}, $S_{21}, etc.$).

Heating and drying processes constitute essential processes of woodworking technologies on MDF-like materials and require a lot of energy. For this reason, knowing the amount of water stored inside the wood's void spices, which is caused by natural reasons such as (relative humidity or rain) or unnatural means (by saturating wood specimen in water) is of great importance in directly affecting the methods and process duration to be applied during fabrication in either drying or heating. Therefore, by determining the amount of water inside during the production stages, energy savings will be possible with the application of high-frequency RF heating technologies [2, 3], and to obtain that much energy efficiency, getting perfect impedance matching as much as possible is an inevitable need. Note that the generator's internal impedance is at one side of the impedance matching, and the impedance of the material under process "$\eta = \sqrt{\mu/\varepsilon}$" is on the other side. Here, ε and μ are the dielectric permittivity and magnetic permeability of materials, respectively [4]. As with all other materials that have water absorbed, there is a direct relationship between the amount of water in natural wood structures and their electrical

properties [5-8]. Dielectric measurements on impregnated wood were performed with various aqueous solutions to investigate the molecular description of water and solvent molecules in the voids [9]. These stimulating studies focus on water saturation in wood structures without requiring any chemical process allowing the cellulosic networks (equivalently, dielectric properties of wood) to be manipulated more easily. Natural wood-based meta-material (NWM) structures light the future of sensor technologies by controlling the moisture content allowing for overcoming the limitation of inherent dielectric properties of natural wood and presenting significantly enhanced microwave absorption performance [10].

The focus of this study is to evaluate and analyze the physical properties of the proposed wooden material through different moisture conditions. Also, expressing the relationship between wood and moisture by generating empiric models in which it will be more beneficial for estimating the dielectric properties and moisture values of the investigated samples. On the other hand, it is possible to estimate the electrical properties of known woods with available water content (briefly refers to its density), or, conversely, to estimate the amount of water absorbed by a wood material with known electrical properties via remote sensing applications. However, a limited number of references will be considered in remote sensing throughout this manuscript since remote sensing applications are not the main aim of this study. Other sub-related studies could be surprisingly found in the literature, wood materials which are classified as well-known biodegradable/recyclable materials. They have begun to play an essential role in the field of the sustainable electronics industry. The possible usage of wood materials (typically their

cellulosic structures) in the electronics industry has become widespread in recent years. A thorough understanding of cellulose's hierarchical structure and unique properties has made it a strong candidate as a PCB (printed circuit board) substrate. During the investigation of wooden material, it has been estimated that wooden structures with a relative permittivity $\varepsilon_r \approx 2.0$ and a relatively small loss tangent "$tan\delta$" values have an excellent opportunity to both increase the quality of data transmission and to achieve high-speed signaling [11-13]. And, typically, controllable features of wood structures have great potential to bring flexible production opportunities in the electronics industry [14-16]. The most significant advantage of wood-based materials with cellulosic structures compared to industrial polymeric materials is having a low density of these materials. This advantage can solve the problems of payloads (due to electronics' PCBs (printed circuit board) and peripherals) associated, especially within the aerospace industry [17, 18]. While the density of well-known polymers changes between 0.92 -1.45 [$g.cm^{-3}$], the thickness of wood structures changes between 0.5-0.85 [mm] [13], which refers to half in weight in comparison.

It has been tried in the literature to determine the electrical properties (refractive index $n = \sqrt{\varepsilon_r}$, where $\varepsilon_r = \sqrt{(\varepsilon')^2 + (\varepsilon'')^2}$) at 1.41 GHz of the leaves of *Betula pendula* tree branches depending on both moisture content and at different temperatures and underlined the importance of them for remote sensing [1]. The increasing moisture content results in increasing dielectric constant (for Pinus Silvestri's var. Mongolia trees) has been reported for low frequencies up to 30MHz, and this variation can be expressed as an empiric mathematical model describing a relationship between the moisture

content and dielectric constant [19]. However, during the wooden material research, the dielectric constant variation with frequency has been studied in discrete/single frequencies in general. In many applications, including sensor design and *RF (Radio frequency)* heating systems, it is necessary to know the tangent loss values of wood-based structures like other typical artificial materials and their relative permittivity. A literature study has a discussion on examining Cryptomeria japonica trees up to 20GHz underlines that water has been strongly constrained inside wood voids such as intercellular spaces and capillaries. Researchers have shown how the relaxation process of free water in wood markedly deviates from that of free water in aqueous solutions of polymers [9].

Meanwhile, another investigation of dielectric properties of *Natural Borneo woods* (keranji, kayu malam, and kumpang*)* was conducted in a 2GHz-6GHz frequency interval. However, throughout the study, no mathematical models have been provided for revealing a relationship between electrical properties and moisture content (equivalently density) [20]. The literature shows a relation between dielectric parameters, moisture content, and mechanical strength of fir and oak wood structures as a mathematical model at one frequency of 9.8GHz [21]. Dielectric properties of atlas-cedar wood up to 1MHz concerning moisture content were studied; unfortunately, there is no mathematical equation expressing a relation between the components of complex dielectric constant and moisture content [22]. Cedar [23] was examined in the frequency range of 3-12 GHz, but still, in the study, there are no mathematical models for the relationship between the electrical properties and moisture content [23]. The moisture content above the fiber saturation point for Japanese

cedar was estimated using the correlation between the specific dynamic Young's modulus and tangent loss. Also, the spectrum of this study is far from the proposed study [24]. Frozen Douglas-fir and white oak woods were investigated as anisotropic dielectric materials and the study concerns modeling anisotropic dielectric heating by radio frequency (*RF*). The electrical permeability of frozen Douglas fir and white oak trees as anisotropic dielectric materials were modeled regarding *RF* heating with a 50 MHz performance. They obtained plots demonstrating real and imaginary parts of dielectric permittivity in variation concerning temperature. The correlation between moisture content and temperature rise in time was also discussed to understand its *RF* heating capability. However, in the present study, no mathematical expressions describe relations between moisture content and dielectric constant, even at 50 MHz [25]. European pine, spruce, and hemlock, which are classified as softwoods, were investigated only at 3 GHz. In the study, for the three-grain directions of the wood, the Authors proposed mainly linear mathematical equations expressing a relation between real and imaginary parts of dielectric permittivity and moisture content. They highlighted that the values observed at the longitudinal values are 2 to 3 times higher than the transverse ones [26]. Blue gum was investigated in terms of complex components of dielectric permittivity in all directions (tangential, radial, and longitudinal) at 2.45 GHz, which is one single frequency. Results were tabulated, but no proposed mathematical expression explains any relation [27].

However, no study was conducted separately or in any combination on Juniper, pine, and cedar in the proposed frequency range. Within the big gap in the literature, the proposed study tries to determine the electrical properties of three different natural wood species widely preferred in Turkey, which are also classified as soft by the wood/forest industry in the 2.17-6 GHz band range. In this study, the proposed wood specimens are classified as softwood, which is the wood species preferred by builders and designers in the construction of houses and during home improvement works [28, 29]. The main contribution that the study reveals when compared to the existing studies in the literature is that mathematical models have been derived for the three natural softwood species studied in a wide frequency interval. The collected S-parameters intend to express the relationship between the complex dielectric constant versus moisture content and density for Juniper, pine, and cedar from the soaked point to the equilibrium point. With this aspect, the study is also unique in literature. The proposed empiric models will allow practically calculating the electrical properties of these natural woods whose density is known without the need for any non-destructive testing system in a later process. During heating or drying in RF systems, these equations can be used as feedback control parameters to make the system energy-efficient and adaptable. In other words, this study aims to provide tools to simplify both the design and application stages of RF heating/drying systems.

2. Theoretical Approach

2.1. Dielectric Permittivity of Materials

The dielectric permittivity is a complex quantity given by Eq.1. While the real part indicates the amount of energy to be trapped by the material, the imaginary part, called the dielectric loss factor, quantifies the material's capability of dissipating electromagnetic energy into heat [30, 31].

$$\varepsilon = \varepsilon' + j\varepsilon'' \qquad \left[\frac{F}{m}\right] \qquad (1)$$

λ_g, d, $\Delta\phi$, and ΔA are, respectively, the operating wavelength in the material, the thickness of the sample, and the phase measured in S_{21} data and amplitude measured in S_{21} data. Eq.2 for the real part (ε') and Eq.3 for the imaginary part (ε'') of the dielectric constant [32, 33].

$$\varepsilon' \simeq \left(1 + \Delta\phi\lambda_g/360d\right)^2 \qquad \left[\frac{F}{m}\right] \qquad (2)$$

$$\varepsilon'' \simeq \Delta A\lambda_g\sqrt{\varepsilon'}/8.686\pi d \qquad \left[\frac{F}{m}\right] \qquad (3)$$

It is considering that the measurements conducted with VNA for the scattering parameters of both, S_{11} and S_{21}, it is more convenient to determine the reflection and absorption coefficients employing Eq.4 and Eq.5, unlike Eq.2 and Eq.3. The Nicholson-Ross Weir method using the scattering parameters is a well-known proven mathematical expression [34]. The reflection coefficients associated with the symbol "Γ" and the transmission coefficient associated with the symbol "T" are the parameters to be reconstructed by using Eq.4 and Eq.5 [34, 35]. Eq.6 is related to the intermediate step solution that gives the transition value X. The resultant reflection coefficient Γ and the consequent transmission coefficient T can be calculated using Eq.7 and Eq.8, respectively [36].

$$S_{11} = \Gamma * (1 - T^2)/(1 - T^2 * \Gamma^2) \qquad (4)$$

$$S_{21} = T * (1 - \Gamma^2)/(1 - T^2 * \Gamma^2) \qquad (5)$$

$$X = (S_{11}^2 - S_{21}^2 + 1)/(2 * S_{11}) \qquad (6)$$

$$\Gamma = X \pm \sqrt{X^2 - 1} \qquad (7)$$

$$T = S_{11} + S_{21} - \Gamma/1 - (S_{11} + S_{21}) * \Gamma \qquad (8)$$

To complete the final calculation, Eq.9 is expressed as the intermediate step solution for magnetic permeability"μ", where L denotes the thickness of material under process and, Λ is the transition parameter.

$$1/\Lambda^2 = -(1/(2 * \pi * L) * \ln(1/T))^2 \qquad (9)$$

Using previously obtained transition parameters, "Λ" and "X", relative magnetic permeability and relative dielectric permittivity are calculated using Eq.10 and Eq.11. In the equations, λ_g denotes the wavelength in the waveguide, for example. λ_0 represents the wavelength in a vacuum. λ_c represents the wavelength at the cut-off frequency. Both relative permeability (Eq.10) and relative permittivity (Eq.11) are unitless quantities.

$$\mu_r = \frac{(1 + \Gamma)}{\left(\Lambda * (1 - \Gamma) * \sqrt{(1/\lambda_0) - (1/\lambda_c)}\right)} \qquad (10)$$

$$\epsilon_r = (\lambda_0^2/\mu_r) * ((1/\lambda_c) + (1/\Lambda^2)) \qquad (11)$$

2.2. Preparation of specimen

In the study, three softwood Juniper (Juniperus excelsa Bieb.), Turkish pine (Pinus brutia), and Lebanon cedar (Cedrus libani) samples were obtained from the Mediterranean region in Turkey. The defect-free small pieces have been classified into three groups according to their physical dimensions to be mounted between waveguide adaptors, as tabulated in Table 1. These are prepared in the form of 62 mm (tangential) x 82 mm (radial) x 4 to 6 mm (longitudinal); 70 mm (tangential) x 100 mm (radial) x 4.5 to 5.0 mm (longitudinal); 95 mm (tangential) x 137 mm (radial) x 4.5 to 5.5 mm (longitudinal). Since the masses of each material at any step are known during the measurement, obtaining the sample density at the appropriate phase was also possible. However, there is an assumption that the wood types and textures,

which vary among wood species, directly influence the electrical properties of samples. It is well known that after wood type (softwood in this study), anatomical and chemical content are two of the most significant variables in the physicochemical properties of wood. These are also clear cases for wood species with different anatomical cell structures and wood-moisture interactions (moisture sorption). Besides the wood type and physical properties (density), major cell-wall constituents of cellulose, lignin, and hemicelluloses are hygroscopic. Their moisture sorption capacity depends on their hydrophilic properties as well as the accessibility of water to the polymer chains. Meanwhile, their textures, as expected naturally, are different from each other in that the water absorption level of each sample varies. These variations directly influence the electrical properties of wood samples.

Table 1. The physical dimension of wood samples

Code		SW1	SW2	SW3
Name		Cedar	Juniper	Pine
Thickness (mm)	WR340	4.5	5.5	4.75
Width x Length (mm)		95x137	95x137	95x137
Thickness (mm)	WR229	4.5	4.75	4.5
Width x Length (mm)		70x100	70x100	70x100
Thickness (mm)	WR159	4	4.5	5.5
Width x Length (mm)		62x82	62x82	62x82

The size of the collected data is 16,500 for each wood sample, which means that 16,500*3=49,500 data in total throughout the study. These data were taken concerning moisture content variation. S_{11} and S_{21} are the data sets that are called raw data throughout the study, and the electrical properties of specimens are the calculated results obtained by employing them.

2.3. Moisture Content Calculation

The proposed wooden material was immersed in water-filled containers to observe the moisture content variation of the selected specimen from the soaked point to the equilibrium point throughout the study. It was kept for a few days until their saturated weights changed. Specimens immersed in water-filled containers during the experimentally determined time interval observed that four days is the most prolonged duration, including a safety margin called the soaked point. Four days later, when the samples were removed from the containers, the measurement process was started, and each specimen was reweighed at every measurement step. The measurement processes continued until the mass of the material was left to air-dry, typically called an equilibrium point. When the measurement campaign was completed, all specimens were taken into a standard oven-drying process to reach oven-dry weight called m_{oven}. Note that the air-dry level in real life, unless any other drying process is not applied, the natural specimen's moisture content is around 12-14% [37]. The moisture content calculated by Eq.12 in the wood below the fiber saturation point (FSP) is composed of bound water (BW), and free water (FW) above FSP. FSP is the moisture content that occurs when the cell walls are saturated with water molecules bound to the walls, and all the cell lumens are empty.

$$MC\% = \frac{(m_{measured} - m_{oven})}{m_{oven}} \, x100 \qquad (12)$$

Wood shrinkage does not begin until FSP is reached when drying an initially soaked wood. Below the FSP, i.e., after all, FW has been evaporated, the specimen loses some BW until it

reaches equilibrium with the environmental conditions determined by relative humidity (RH) and temperature (T). The two regimes below and above the FSP, i.e., BW and FW, have different electrical and dielectric properties that are also temperature-dependent. The distinction between BW and FW regimes is not considered in the paper, nor is the dependency on T. This information is illustrated in Fig.1. This study did not consider variations concerning room temperature and relative humidity.
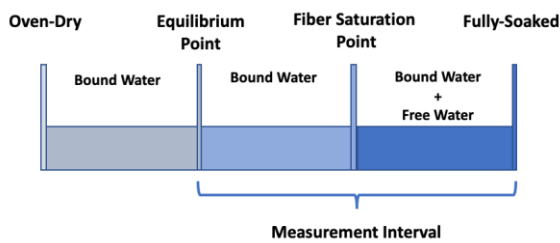
Figure 1. Measurement Interval

2.4. Measurement Campaign

In this study, the previously approved measurement methods and setups were conducted [5-7, 38-40], and the specimen dimension concerning both the used wavelength and moisture content is not expected to cause any uncertainties. As in the previous studies, it is necessary to control the amount of humidity in the working environment when working with materials whose weight changes due to the humidity of the environment, such as wood. It is reported that in heated homes in mid-Sweden, the moisture content in wood averages out across the year at 7.5%, with the highest figures in summer (7–12%) and the lowest in the winter (2–6%)[41]. In this sense, the limitations of the proposed study, the room's humidity level was kept in the range of 30%-50%, the room temperature was maintained between 24 ∓ 2 ℃ throughout the study, and all weight

measurements were done with a 0.001-gram accuracy scale. Fig. 2a, 2b, and 2c demonstrate the components of the measurement campaign.

(a) Measurement process
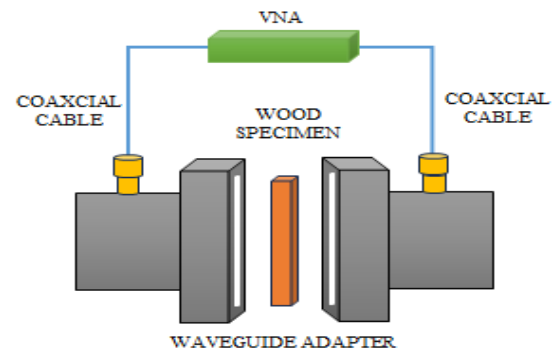
(b) Measurement Diagram

(c) Specimen Texture and Immersion State

Figure 2. Measurement Campaign

2.5. Test Setup

Three standard waveguides and compatible adapters covering the frequency range 2.17 GHz - 3.3 GHz, 3.3 GHz - 4.9 GHz, and 4.9 GHz-7.1 GHz are used to cover the frequency range used.

These waveguides are connected to a vector network analyzer (VNA) whose operating frequency is limited by 6GHz, the specimen is neatly placed in the adapter, and measurements are carried out. The photograph of the setup where the measurements were made is given in Fig.2a. Each day, 2–3 measurement campaigns, including both weight check (current water content) and complex S-parameter (reflection and transmission coefficient) measurements, were held.

3. Results and Discussion

In this section, results and their obtaining mechanism steps are explained step by step. In subsection 3.1, the effect of dielectric permittivity measurement and moisture content on dielectric properties are shown. While in subsection 3.2, results obtained from subsection 3.1 are used to generate linear models. These models are ensuring to reach one of the main aims of this study is to suggest these models could be used for fast and easy determination of dielectric properties for wood materials in industry. Loss tangent value is important and is related to the RF heating capabilities of the material. A higher tangent value represents the relatively higher RF energy conversion into heat in materials. Subsection 3.3 investigates measured loss tangent values, and models are generated using measured values. Proposed models show characteristics of loss tangent along frequency range that could be used by an industry professional to optimize and tune RF heating systems. Subsection 3.4. is a perspective for all loss tangent values in any density and frequency. These results can be used to explain how the behavior of loss tangent values varies towards different moisture and density conditions along the frequency range.

3.1. Calculated Dielectric Permittivity

The selected data plot shared in this section represents relative dielectric permittivity "ε_r" variation concerning frequency considering moisture content, which is calculated by using Eq.11. On the plots in Fig. 3a, 3b, 3c, 3d, 3e, 3f, 3g, 3h, and 3i legends and/or codes WR340, WR229, and WR159 are for waveguides operating at 2.17-3.3 GHz, 3.3-4.9 GHz, and 4.9-7.1 GHz frequency intervals, respectively. Since the upper limit of VNA in the laboratory is 6.0 GHz, data collection ended at 6.0 GHz. The variation of ε_r concerning both frequency and moisture content for the juniper tree is on the plot. The mathematical relationships representing the relation between relative dielectric permittivity and moisture content are discussed in Section 4.2. When Fig. 3a, 3b, 3c, 3d, 3e, 3f, 3g, 3h, and 3i are carefully examined by considering whole frequency ranges that worked on and any moisture content ratio, the highest average dielectric permittivity constant is obtained for pine woods. The lowest value is for juniper wood. The value of cedar is in between them but close to juniper woods. In the lower band, the relative permittivity of pine wood reaches~35, cedar is near~16, and Juniper is close to ~11. These deviations imply that the technical approaches must differ when these samples must be subjected to the electromagnetic field to develop RF heating systems or other sensor technologies. From the plots, one may observe that examples having a moisture content of less than 3% cannot be distinguishable. As noted earlier, air-dry level refers to the moisture content of natural wood samples under normal conditions that are not less than 10 % - 14 % [41].
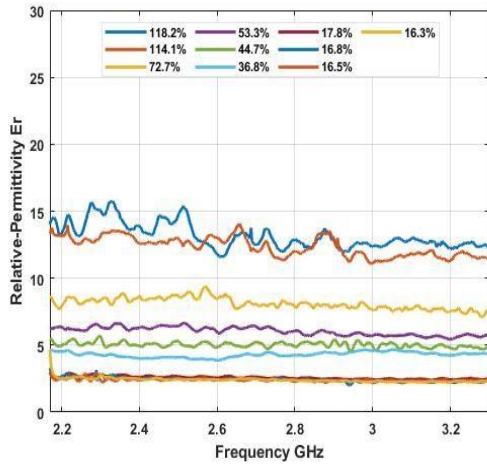
(a) 2.17GHz-3.3GHz for Cedar
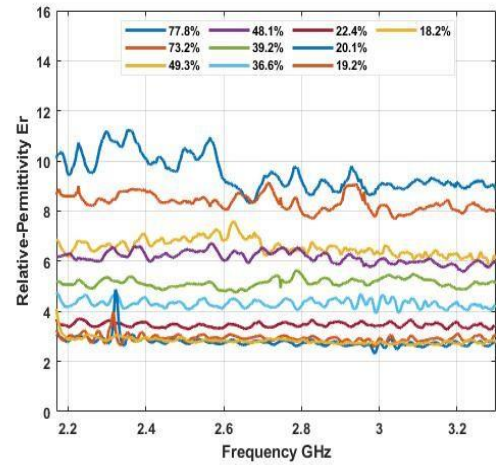
(d) 2.17GHz-3.3GHz Juniper
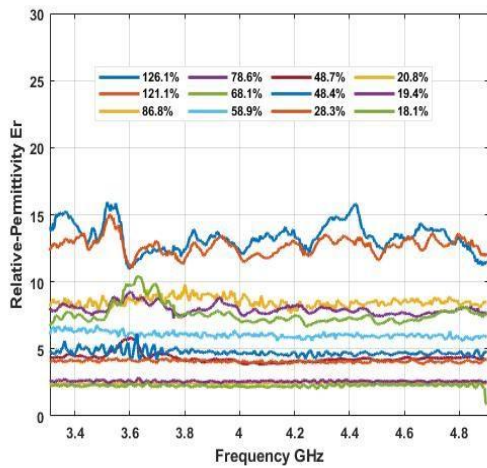
(b) 3.3GHz-4.9GHz for Cedar
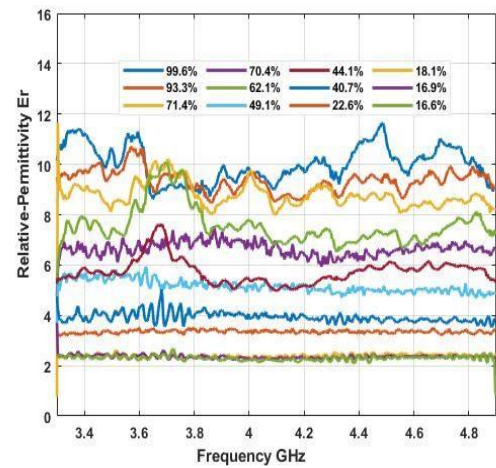
(e) 3.3GHz-4.9GHz for Juniper
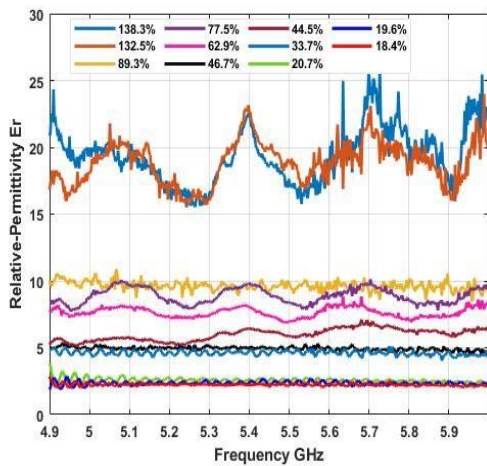
(c) 4.9GHz-6.0GHz for Cedar
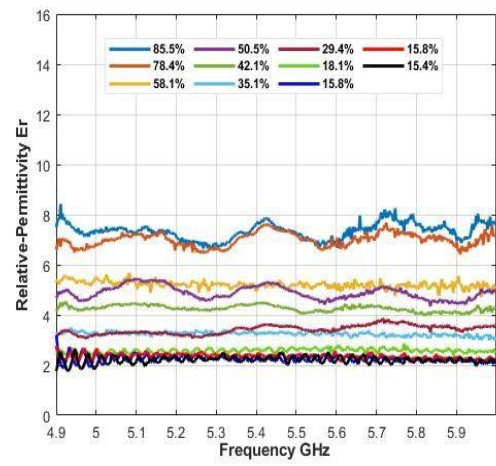
(f) 4.9GHz-6.0GHz for Juniper
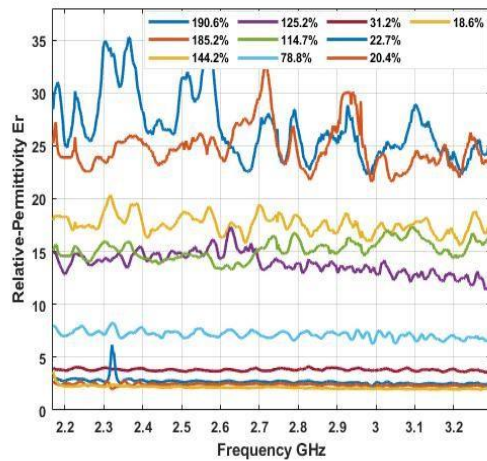
(g) 2.17GHz-3.3GHz for Pine
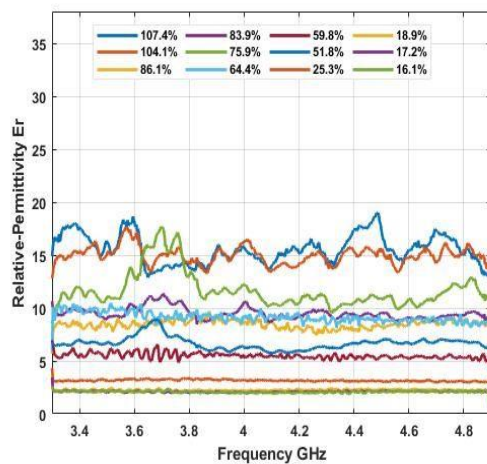
(h) 3.0 GHz-4.9GHz for Pine
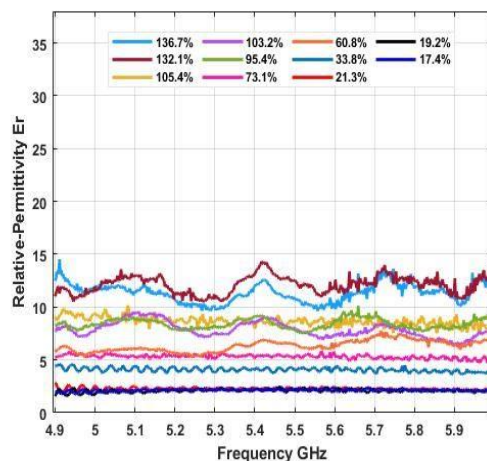
(i) 4.9GHz-6.0GHz for Pine

Figure 3. Relative dielectric permittivity of softwoods

3.2. Mathematical Model Relative Permittivity and Moisture Relation

Each part of the circular rings shown in Fig.4a, 4b, 4c, 4d, 4e, and 4f represents an average of 500 raw data. Since plots end where the soaked specimen cannot immerse in the water anymore, there is no data or model response beyond that level. Higher limits of the horizontal axis of all plots are because of the maximum water absorption capacity of the different specimens. Fig. 4a, 4c, and 4e are for relative dielectric permittivity variation concerning moisture content, and Fig. 4b, 4d, and 4f are for relative dielectric permittivity variation regarding density. For most practical industrial applications, density plots can be more beneficial since the volume and weight of specimens are measured simultaneously. Such a plotting method was proffered to avoid confusion/crowding in the resulting graphics. Where in the legends end with 340, 229, and 159 of all figures stand for 2.17-3.3 GHz, 3.3-4.9 GHz, and 4.9-7.1 GHz standard waveguides, respectively. Linear mathematical models expressing the relationship between moisture content and average dielectric permittivity are given. Root mean square errors for selected wood samples are better than 0.92 in general, for low-frequency interval $R^2 \to 0.99$, and higher frequency interval $R^2 \to 0.92$. The fact that the R square value is more significant than 0.9 "$R^2 > 0.9$" is essential in showing the strong competence of the obtained equations to represent the expected relationships. It is possible to generate one single mathematical representing the whole band response for each wood structure, but estimation capability will decrease in that scenario. In the case of knowing moisture content or equivalency density, these mathematical models allow application engineers to calculate the relative dielectric

constant of cedar, Juniper, and pine without using any non-destructive methods.

(a) Cedarwood

(b) Cedarwood
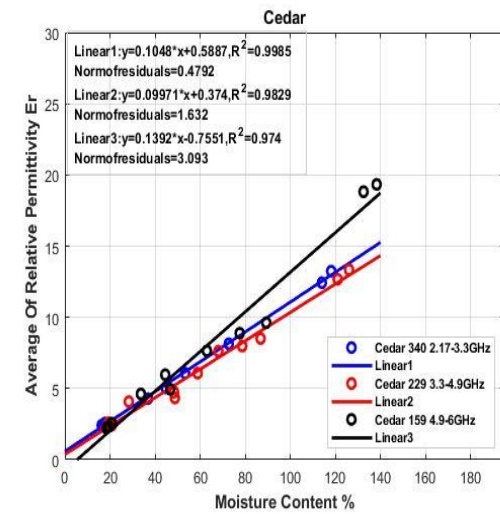
(c) Juniper wood
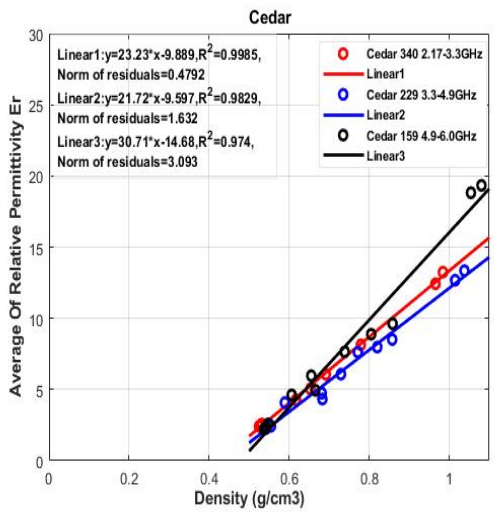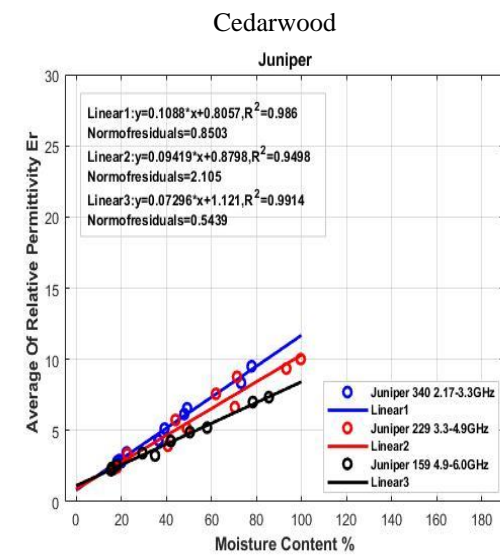
(d) Juniper wood
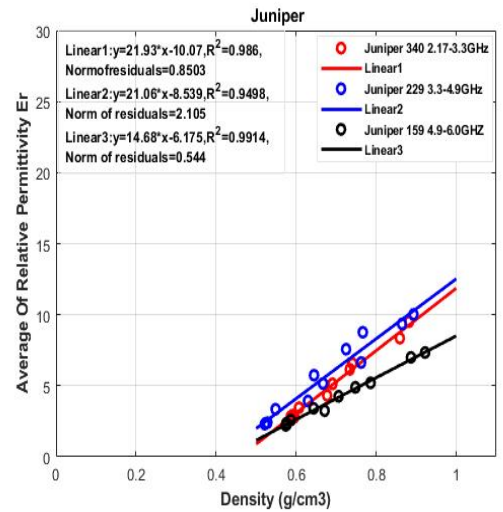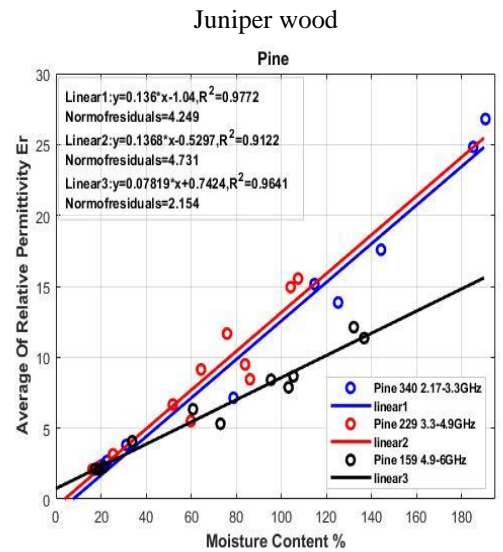
(e) Pine Wood

(f) Pine Wood
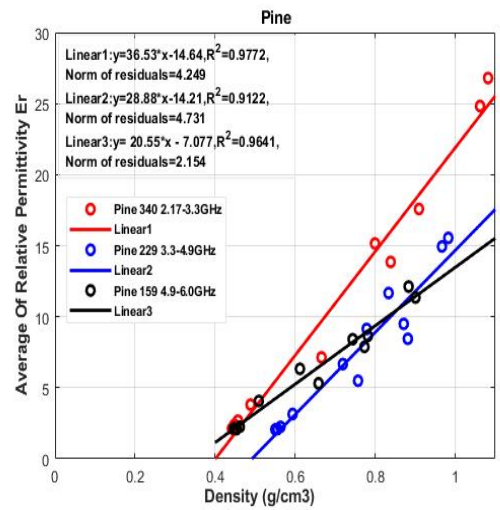
Figure 4. Relative Permittivity and Moisture Relation

3.3. Mathematical Model Loss Tangent and Moisture Relation

Fig. 5a, 5b, 5c, 5d, 5e, and 5f show the variation of loss tangent values of pine, cedar, and juniper trees depending on moisture content and density. The answers of each specimen corresponding to 3 different sub-bands (2.17-3.3 GHz, 3.3-4.9 GHz, and 4.9-6.0 GHz) are shown on the same plot. Each figure ring shows the average values obtained corresponding to 500 different frequency points along the relevant band at the indicated humidity value. At this point, it is helpful to remember that each of the 500 different values is another multiple data average taken at different time intervals to minimize measurement error.

Three different mathematical models valid in three different waveguides are given for both moisture and density variation, and models seem to work appropriately to describe selected wood specimens. It has already been predicted that cedar has considerably higher lignin (35.7 %) and extractive (11.9 %) but lower holo-cellulose (52.4 %) content than Black pine (Pinus nigra, Arnold. This could contribute to its uncommon loss of tangent properties[42]. Fig 5a shows the tangent loss variation concerning moisture content for the cedar-wood samples; the models mainly take an arc shape at both 2.17-3.3 GHz and 3.3-4.9 GHz frequency intervals, while the response is a sinusoidal shape at 4.9-6.0 GHz frequency interval. Fig 5b demonstrates the loos tangent variation of the juniper wood specimen; a sinusoidal-like harmonic movement is observed for both the frequency intervals 3.3-4.9 GHz and 4.9-6.0 GHz, delayed form of that harmonic movement is observed in 2.17-3.3 GHz frequency interval. Fig 5c shows the loss tangent results for the pine specimen with almost the exact response shape in the whole frequency interval worked on.

Moisture content up to 20 % can be assumed as their natural level, and the average loss tangent value is around 0.2. Observed that $R^2 \rightarrow 0.75$ is in the worst case and $R^2 \rightarrow 0.91$ is in the best. All equations can be used to calculate loss tangents within a particular level error. Fig 5d, Fig 5e, and Fig 5f show the tangent loss variation concerning density for cedar wood, juniper wood, and pine wood, respectively. Responses are similar and have arc shape responses; models have that R^2 better than 0.75 for each specimen and each band interval.

Model 1 = (-0.5633*x^2 + 91.35*x + 539.4) / (x +1.534e+04)

Model 2 =(-0.07064*x^2 + 11.61*x + -15.38) / (x +1664)

Model 3 = 0.2395*exp(-((x+0.4065)/0.6091)^2) +0.2361*exp(-((x-1.619)/1.326)^2)

(a) Cedar Wood

Model 1= (-1898*x^2 + 3089*x - 969) / (x + 1043)

Model 2 = (-14.83*x^2 + 24.81*x + -8.334) / (x +6.894)

Model 3= 0.2248*exp(-((x-0.9636)/0.6104)^2)
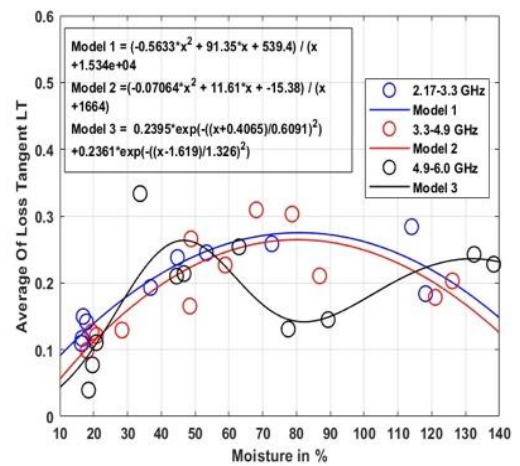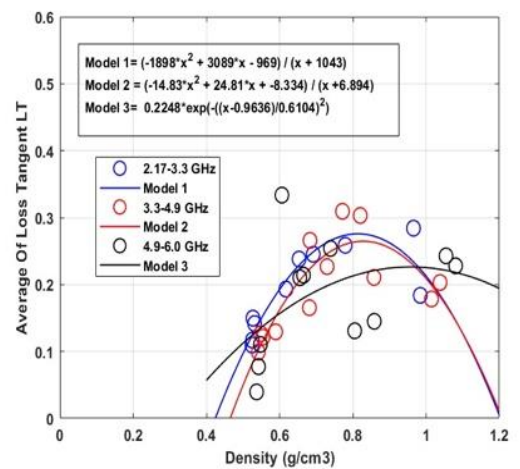
(b) Cedar Wood
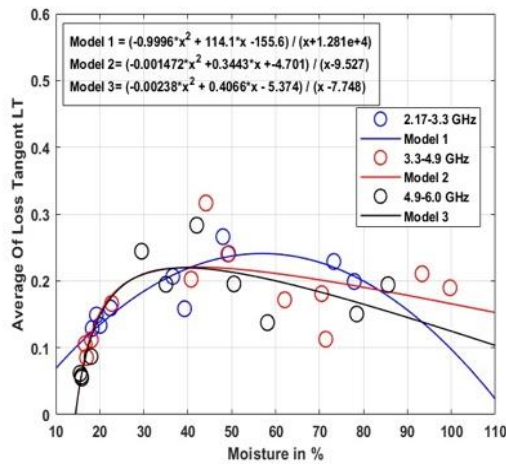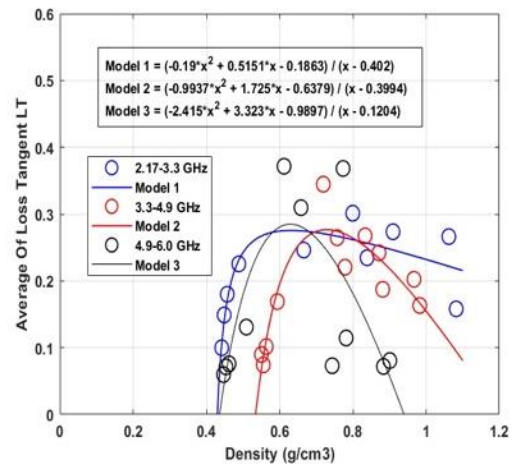
(c) Juniper Wood

(f) Pine Wood

Figure 5. Loss Tangent and Moisture Relation
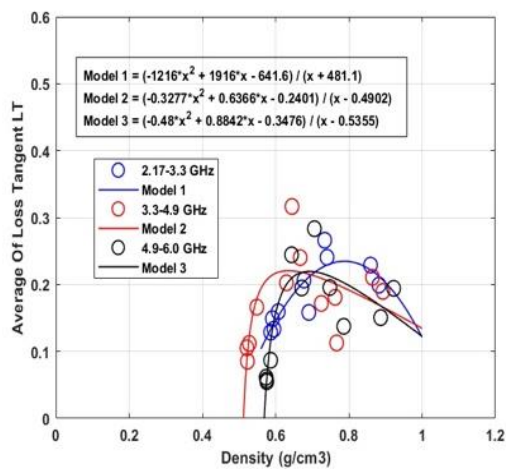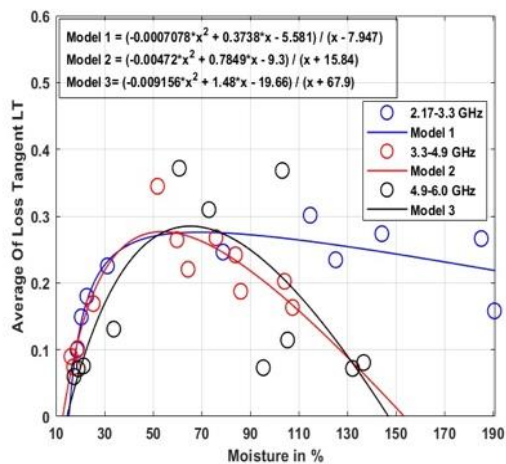
3.4. Loss Tangent versus Density

Fig. 6a, 6b, 6c, 6d, 6e, 6f, 6g, 6h, and 6i are for loss tangent "tanδ" variation of cedar, Juniper, and pine woods considering density and frequency. When the figures are examined, a higher tanδ value is observed in the case where the density of the specimen is high, and the frequency of the related sub-band is low. Remember that the performance of RF heating/drying systems is susceptible to materials' conductivity (equivalently to tanδ) described in terms of moisture content. In practical usage, density can be easily calculated using mass and volume in contrast moisture content calculation needs more effort. In light of this fact, moisture content can be replaced by density to simplify the process. As the importance of loss tangent is highlighted in the Introduction, these relations/responses on plots can be used as feedback control parameters to make the system energy-efficient and adaptable. The average value of tangent loss for all specimens for whole band intervals is around 0.2.

(d) Juniper Wood

(e) Pine Wood
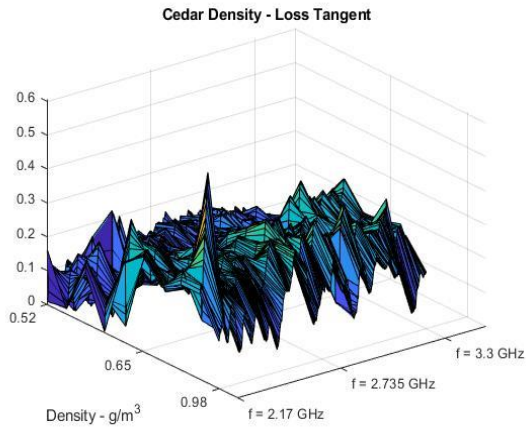
(a)WR340 Cedar
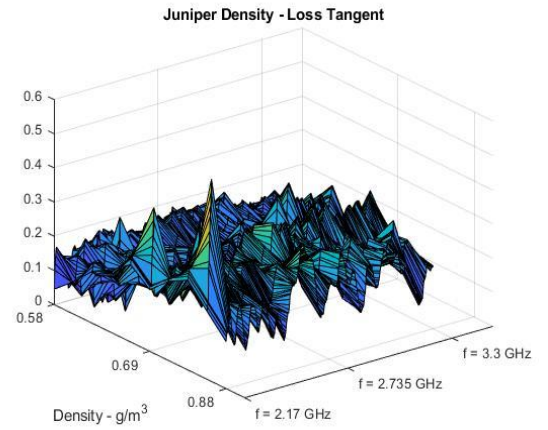
(d)WR340 Juniper
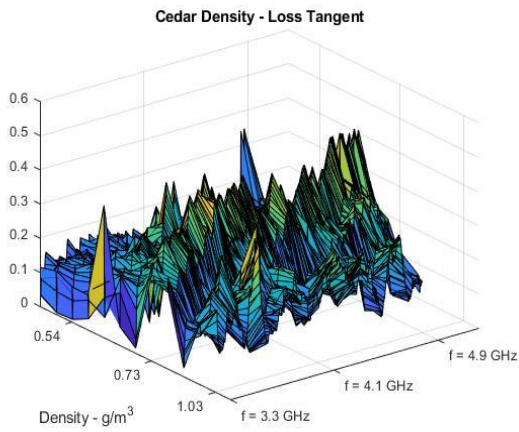
(b)WR229 Cedar
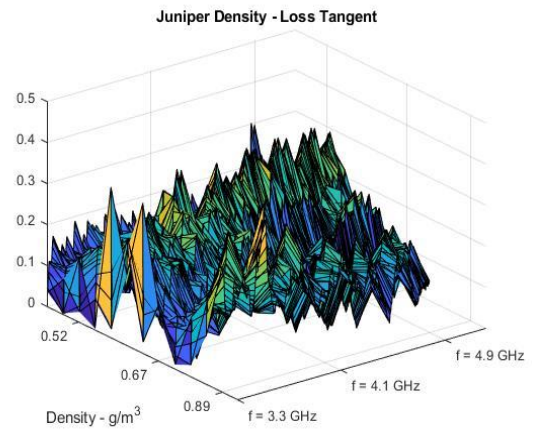
(e)WR229 Juniper
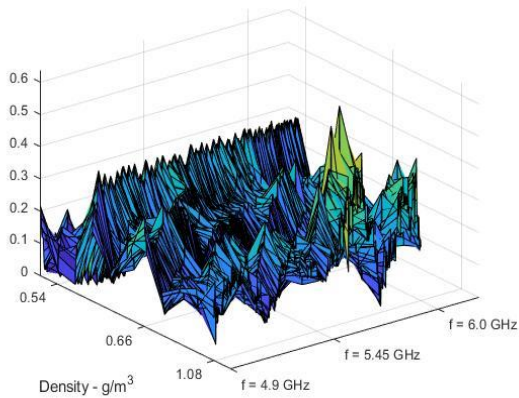
(c)WR159 Cedar

(f)WR159 Juniper

(g)WR340 Pine

(h)WR229 Pine

6i)WR159 Pine
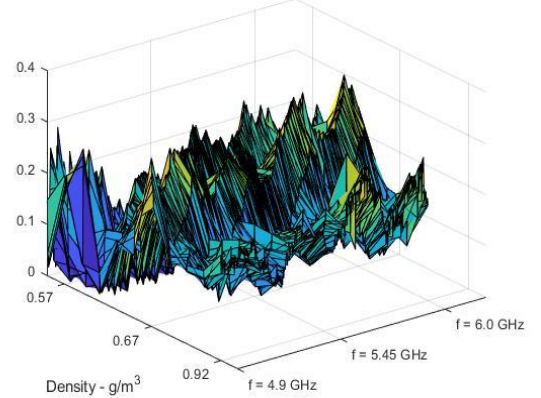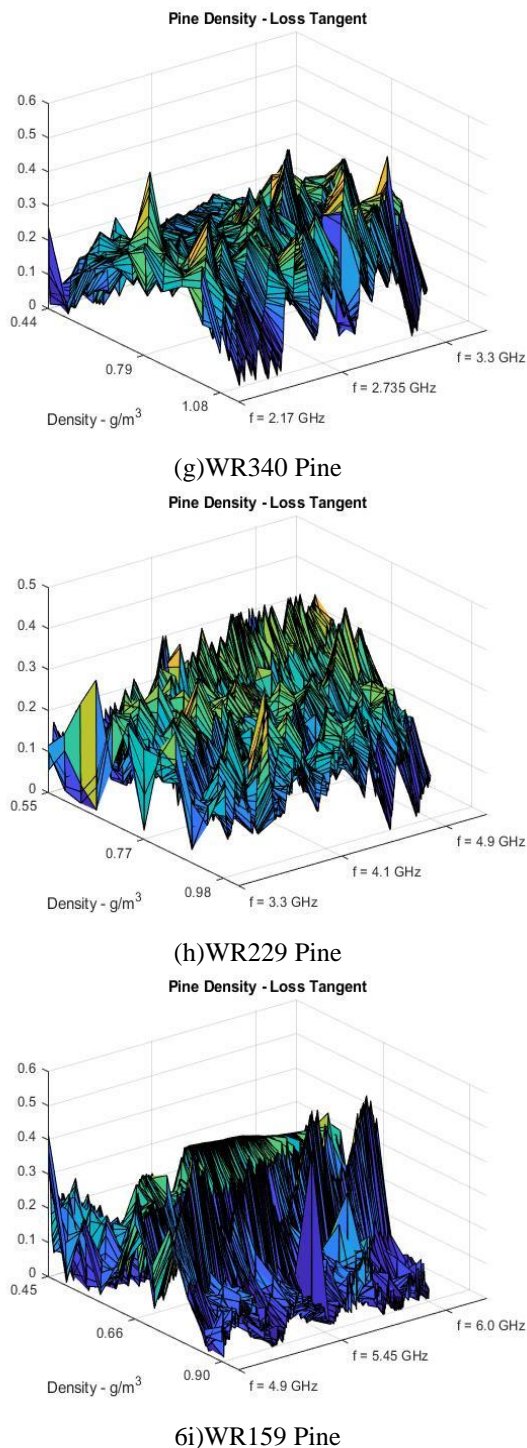
Figure 6. Softwood Loss Tangent and Density Relation

4. Conclusions

This study investigates well-known natural softwood specimens (Cedar, Juniper, and Pine) while considering the selection of wood specimens without any knots/defects.

Limitations of the proposed study are the selected frequency range between 2.17-6.0 GHz which could have been expanded and non-comparable moisture content levels. The saturated wood specimens have different moisture content levels depending on their texture and water absorption capacity (i.e., pine wood reaches above 180%, cedar is 140 %, and Juniper is 100 %, while specimens' wood densities vary between 0.4-1.2 [g/cm^3]. The equilibrium moisture content (EMC) was the stopping point of the measurement campaign because most of the common wood processing activities happen above the EMC point. In this research, as a non-destructive microwave measurement technique a VNA (victor network analyzer) was applied to calculate the S-parameters of wooden material during different moisture conditions. While using the collected S-parameters data in calculations of both relative permittivity and tangent loss, an empiric model generation was possible for expressing the relation between moisture and dielectric and moisture and tangent loss. The Proposed empiric models for relative dielectric permittivity versus moisture content and versus density have a value of $R^2 > 0.9$, and empiric models of tangent loss have $R^2 > 0.75$. So, these models can represent prescribed relations. Briefly, the proposed models to calculate the electrical properties of a wood specimen do not require any additional s-parameter measurements for further applications. The proposed models present an opportunity window for adaptively controlling RF-based wood processing industries.

For future work; artificial intelligence models will be constructed to improve the accuracy and reliability of proposed models. The second critical step will be implementing tuned models to real RF heating/drying systems as dynamic

control parameters. Expanding the study to cover other wood structures used in the forest industry will also be a critical step for the wood industry.

The effect of knots/defects requires an additional effort that will broaden the study's content. Also, using wood structures as sustainable electronic substrates will be more beneficial for the electronic industry. How the chemically immersed operation changes the electrical properties of the natural wood is also a potential future work. Relative humidity (*RH*) and temperature (*T*) effects determining the equilibrium moisture content form our agenda to expand proposed studies further.

Acknowledgments

Conflict of interest

The authors declare that there are no conflicts of interest regarding the publication of this manuscript.

Author Contribution Statement

Author Sinan Alsaadi: helped by providing this study with the required wood materials while working on the measurement process for collecting the S-parameters needed for this research with preparing and analyzing the data pool for generating empiric models for expressing the relation between dielectric results and moisture variations (also for density), also writing this study manuscript. Author Selcuk Helhel: proposed this research problem and supervised the findings of this work, providing this research with the measurement tools needed in Akdeniz University EMUMAM lab facilities and also helping in writing this study manuscript. Author Atalay Kocakusak: helped this study with the required wood material and also contributed to data collection, analysis, and empiric model generation.

5. References

1. Romanov, *A. Some Behavior Features of Dielectric Properties of Water in Birch Wood at a Frequency of 1.41 GHz,* IEEE Transaction on Geoscience and Remote Sensing, Vol. 60, 2022. https://doi.org/10.1109/TGRS.2022.3157642

2. Wang D., Xianjun H., Lv J. and Chen X., 2022. *The Effects of Moisture and Temperature on the Microwave Absorption Power of Poplar Wood Forests,* Vol. 13, pp. 1-12. https://doi.org/10.3390/f13020309

3. Pereiraa, C. M., Blanchard C., Carvalhoa L. M. and Costa C. A.,2004. *High-frequency heating of medium density Fberboard (MDF): theory and experiment*, Chemical Science Engineering, Vol. 59, pp. 735-745. https://doi.org/10.1016/j.ces.2003.09.038

4. Helhel S., 2019. *Microwave Techniques (in Turkish)*, 1 ed., Istanbul: Nobel,.

5. Kocakusak A., Colak B., and Helhel S., 2016. *Frequency-dependent complex dielectric permittivity of rubber and magnolia leaves and leaf water content relation.* Journal of Microwave Power and Electromagnetic Energy, Vol. 50, Issue. 4, pp. 294-307. https://doi.org/10.1080/08327823.2016.1254135

6. Genç A., Basyigit I. B., Dogan H. and Colak B.,2021. *Measuring and modeling the complex-permittivity of the hemp plant (Cannabis Sativa) at X band for microwave remote sensing*, Journal of Electromagnetic Waves and Applications, Vol. 35, Issue. 14, pp. 1909-1921. https://doi.org/10.1080/09205071.2021.1924294

7. Metlek S., Kayaalp K., Basyigit I. B., Genc A., and Dogan H. 2021. *The dielectric properties prediction of the vegetation depends on the moisture content using the deep neural network model*. International Journal of RF and Microwave Computer-Aided Design, Vol. 31, Issue. 1. https://doi.org/10.1002/mmce.22496

8. Dogan H., I. Basyigit B. and Genc A., 2020. *Determination and modeling of dielectric properties of the cherry leaves of varying moisture content over 3.30-7.05 GHz frequency range*. Journal of Microwave Power and Electromagnetic Energy, Vol. 54, Issue. 3, pp. 254-270,. https://doi.org/10.1080/08327823.2020.1794724

9. Sudo S., Suzuki Y., Asano M., and Yagihara S., 2022. *Investigation of the molecular description of small molecules in void spaces of wood using dielectric measurements* Wood Science and Technology, Vol. 56, pp. 1887-1902. https://doi.org/10.1007/s00226-022-01433-7

10. Quan P. Long C., Zhou J. He X., Liu Y., eVallanceD. D, Li X. and Xie X., 2021. *Natural wood-based metamaterials for highly efficient microwave absorption*

Holzforschung, Vol.. 76, Issue. 4, pp. 368-379. https://doi.org/10.1515/hf-2021-0088

11. Fang Z., Zhang H., Qiu S., Kuang Y., Zhou J., Lan Y., Sun C., Li G., Gong S., and Ma Z., 2021. *Versatile Wood Cellulose for Biodegradable Electronics* Advanced Materials Technologies, Vol. 6, pp. 1-18,. https://doi.org/10.1002/admt.202000928

12. Dobson M., DeLaSierra R. and Christensen N., 1991. *Spatial and temporal variation of the microwave dielectric properties of loblolly pine trunks* in Annual International Geoscience and Remote Sensing Symposium IGARSS '91, Espoo. https://doi.org/10.1109/IGARSS.1991.579264

13. Kokkonen M. Nelo M, Liimatainen H., Ukkola J., Tervo N., Myllymäki S., Juuti J., and Jantunen H., 2022. *Wood-based composite materials for ultralight lens antennas in 6G systems*. Materials Advances, No.. 3, pp. 1687-1694. https://doi.org/10.1039/D1MA00644D

14. Fu Q., Chen Y. and Sorieul M. 2020. *Wood-Based Flexible Electronics*, ACS NANO, Vol. 14, Issue. 3, pp. 3528-3538. https://doi.org/10.1021/acsnano.9b09817

15. Wang T., Liu S., Hu Y., Xu Z., Hu S., Li G., Xu J., Wang M., Zhang J., Yu W. and Ma X., 2022. *Liquid Metal/Wood Anisotropic Conductors for Flexible and Recyclable Electronics*, Advanced Materials, Vol. 9, pp. 1-12,. https://doi.org/10.1002/admi.202200172

16. Hongli Z., Luo W., . Chiesielski P. N, Fang Z., Zhu J., Henrikson G., Himmel

M., and Liangbing H., 2016. *Wood-Derived Materials for Green Electronics, Biological Devices, and Energy Applications*, Chemical Reviews, Vol. 116, Issue. 16, pp. 9305-9374,. https://doi.org/10.1021/acs.chemrev.6b00225

17. Gerke R., Shapiro A., and Peters D., 2003. *Use of plastic commercial off-the-shelf (COTS) microcircuits for space applications*, in International Electronic Packaging Technical Conference. https://doi.org/10.1115/IPACK2003-35351

18. Cai Y., Zhenyu G., Chakraborty I., Briceno S., and Mavris D., *System-Level* 2018. *Assessment of Active Flow Control for Commercial Aircraft High-Lift Devices*, Journal of Aircraft, Vol. 55, Issue. 3, pp. 1200-1216. https://doi.org/10.2514/1.C034401

19. Xu C., Chai H., Cao T., Cai M., Cai Y. and Liu H., 2019. *Detection of Dielectric Constant of Pinus Sysvestris Var. Mongolia and şts Influencing Factors*. Biosources, Vol. 14, Issue. 2, pp. 4532-4542,. https://doi.org/10.15376/biores.14.2.4532-4542

20. Jayamani E., Rahman R. M., Hamdan S., Kyari M. I., Bin Bakri M. K., Khairuddin S. and Khan A., 2020. *Dielectric Properties of Natural Borneo Woods: Keranji, Kayu Malam, and Kumpang*. Bioresources, Vol.. 15, Issue. 4, pp. 7815-7827. https://doi.org/10.15376/biores.15.4.7815-7827

21. Kol H. S. and Yalcin İ., 2015. *Predicting Wood Strength using Dielectric Parameters*, Biosrources, Vol. 10, Issue. 4, pp. 6496-651,. https://doi.org/10.15376/biores.10.4.6496-6511

22. Hakam A., Chantoufi A., El Imame N., Guelzim M., Ziani M., Famii A., Dirissi-Bakhkat S., Ghailane F., HacmM. i, Sesbou A. and Merlin A., 2017. *Dielectric Properties of Atlas Cedar Wood at its Early Stage of Decay,* International Journal of Pharmacognosy and Phytochemical Research, Vol. 9, Issue. 3, pp. 444-448.

23. Suslyaev V., Kochetkova T., Korovin E. and Volchkov S., 2013. *Spectra of permittivity of different woods in the frequency range of 3–12 GHz*, Sevastopol, Ukraine,.

24. Toshiyuki F., Yanase Y., Sawada Y. and Fuji Y., . *Estimations of the moisture content above the fiber saturation point in sugi wood using the correlation between the specific dynamic Young's modulus and tangent loss*, Journal of Wood Science, Vol. 66, Issue. 1. https://doi.org/10.1186/s10086-020-01879-y

25. Erchiqui F., Annasabi Z., and Diagne M., 2022. *Investigation of the radiofrequency heating of anisotropic dielectric materials with a phase change: application to frozen Douglas-fir and white oak woods*, Wood Science and Technology, Vol. 56, Issue. 1, pp. 259-283. https://doi.org/10.1007/s00226-021-01345-y

26. Peyskens E., Depourcq M., Steven M. and Schalck J., 1984. *Dielectric-Properties of Softwood Species at*

Microwave- Frequencies., Wood Science and Technology, Vol. 18, Issue. 4, pp. 267-280,.
https://doi.org/10.1007/BF00353363

27. Daian G., Taube A., Birnboim A., Shramkov Y., and Daian M., 2005. *Measuring the dielectric properties of wood at microwave frequencies*, Wood Science and Technology, Vol. 39, Issue. 3, pp. 215-223.
https://doi.org/10.1007/s00226-004-0281-1

28. Master Class, "Masterclass," 2021. [Online]. Available: https://www.masterclass.com/articles/types-of-hardwood. [Accessed 05 March 2023].

29. Bond B. and Hammer P., 2002. *Wood Identification for Hardwood and Softwood Species Native to Tennessee*, Agricultural Extension Service, Knoxville.

30. Tornonikov G. I., 1993. *Dielectric Properties of Wood and Wood-Based Materials*, Springer.

31. Hussein W. J. and Hameed K. R., 2022. *Finite-Element Calculation Of Electromagnetic Forces In The Deferent Shapes Of Distribution Transformers Winding Under Short Circuit Condition*, Journal of Engineering and Sustainable Development, Vol. 26, Issue. 3, May.
https://doi.org/10.31272/jeasd.26.3.6

32. Trabelsi S., Kraszewski A. and Nelson S., 2000. *Phase-Shift Ambiguity In Microwave Dielectric Properties Measurements*." IEEE Trans Instrum Meas*., Vol. 49, p. 56–60.
https://doi.org/10.1109/19.836309

33. Kraszewski A. and Nelson S., 2004. *Microwave permittivity determination in agricultural products*., Microw Power Electromagn Energy*, Vol. 39, p. 41–52.
https://doi.org/10.1080/08327823.2004.11688507

34. Jarves J. B., Jenezic M. D., Riddle B. F., Johnk R. T., Kabos P., Christopher L. H., Geyer R. G., and Grosvenor C. A., 2005. *Measuring the Permittivity and Permeability of Lossy Materials: Solids, Liquids, Metals, Building Materials, and Negative-Index Materials, Boulder*: National Institute of Standards and Technology - NIST,. [Accessed online 2023]
https://nvlpubs.nist.gov/nistpubs/Legacy/TN/nbstechnicalnote1536.pdf

35. Ahmed S., Chandra M., and Abdul Hassain, Z. A. 2022. *Reducing The Cross-Polarizationpatternina Dual-Polarized Antenna Using Spiral And Splitting Resonators*, Journal of Engineering and Sustainable Development, Vol. 26, Issue. 6, pp. 30-38, November.
https://doi.org/10.31272/jeasd.26.6.4

36. Balanis C. A., 2012. *Advanced engineering electromagne*tics, John Wiley & Sons.

37. Reeb J. and Brown T. D. 2016. *Air- and Shed-Drying Lumber*, August. [Online]. Available: https://catalog.extension.oregonstate.edu/em8612/html#:~:text=Air%2Ddrying%20means%20stacking%20lumber,months%20to%20almost%20a%20year. [Accessed 08 February 2023].

38. Helhel S., Colak B. and Ozen S., 2009. *Measurement of Dielectric Constant of Thin Leaves by Moisture Content at*

4mm Band, Progress in Electromagnetics Research Letters*,* Vol. 7, pp. 183-191, https://doi.org/10.2528/PIERL09021605

39. Helhel, Selcuk, Kocakusak A. and Sunel M., 2020. *Determining loss tangent values of dry granite for potential S-band applications*, Microwave and Optical Technology Letters*,* Vol. 62, Issue. 11, pp. 3476-3484. https://doi.org/10.1002/mop.32494

40. Saedi T., İsmail I., Alhawari A. R., and Wen W. P., *Near-Field And Far-Field Investigation Of Miniaturized Uwb Antenna For Imaging Of Wood*, AIP Advances, Vol. 9, pp. 1-21, 19 March 2019. https://doi.org/10.1063/1.5081762

41. Ågren A. R., 2021*Swedish Wood,*. [Online]. Available: https://www.swedishwood.com/wood-facts/about-wood/wood-and-moisture/. [Accessed 17 January 2023].

42. Sahin H. T. 2008. *Wood-Water Interactions As Affected By Chemical Constituents Of Woods,* Asian Journal of Chemistry*,* Vol. 20, Issue. 4, pp. 3267-3276.